OPEN

PRS GLOBAL OPEN

ORIGINAL ARTICLE
Research

Hemodynamics and Vascular Histology of Keloid Tissues and Anatomy of Nearby Blood Vessels

Shigeyoshi Eura, MD
Junichi Nakao, MD
Takeshi Iimura, MD, PhD
Shizuko Ichinose, PhD
Chiemi Kaku, MD
Teruyuki Dohi, MD, PhD
Satoshi Akaishi, MD, PhD
Mamiko Tosa, MD, PhD
Rei Ogawa, MD, PhD, FACS

Background: Keloids are red, invasive scars that are driven by chronic inflammation in the reticular dermis. The role of blood vessels in keloid behavior remains poorly understood. In the present study with 32 keloid patients, we examined the hemodynamics of keloid tissue, the anatomy of the blood vessels feeding and draining the keloids, and the vascular histology of keloids.
Methods: Ten patients with large anterior chest keloids underwent near-infrared spectroscopy, which measured regional saturation of oxygen and total hemoglobin index in the keloid and surrounding skin. Another 10 patients with large chest keloids and three healthy volunteers underwent multidetector-low computed tomography. The extirpated chest keloids of 12 patients were subjected to histology with optical, CD31 immunohistochemical, and electron microscopy.
Results: All keloids had a low regional saturation of oxygen and a high total hemoglobin index, which is indicative of blood congestion. Multidetector-low computed tomography revealed dilation of the arteries and veins that were respectively feeding and draining the keloid leading edge. Hematoxylin-eosin staining and CD31 immunohistochemisty revealed considerable neovascularization in the keloid leading edge but not in the center. Electron microscopy showed that the lumens of many vessels in the keloid center appeared to be occluded or narrowed.
Conclusions: Keloids seem to be congested because of increased neovascularization and arterial inflow at the leading edge and blocked outflow due to vascular destruction in the center. The surrounding veins seem to expand in response to this congested state. Methods that improve the blood circulation in keloids may be effective therapies. *(Plast Reconstr Surg Glob Open 2022;10:e4374; doi: 10.1097/GOX.0000000000004374; Published online 10 June 2022.)*

INTRODUCTION

Keloids are abnormal scars that grow relentlessly into the healthy adjacent skin. They remain difficult to manage despite recent advances in the field[1,2]; new diagnostic, preventive, and therapeutic strategies are needed. Because these scars are characterized by persistent chronic inflammation in the reticular dermis due to abnormal wound healing,[1] a key preventive/therapeutic approach may be to suppress this aberrant inflammation.[2] Moreover, given that the inflammatory cells and factors in the wound/scar bed are largely derived from the circulation via the blood vessels, the blood vessels or associated processes could potentially serve as new keloid management targets.

However, our current understanding of keloid hemodynamics, the vessel anatomy around keloids, and the vascular architecture inside keloids remains very limited.[3–5] To date, histological studies and clinical observations suggest that the blood flow in the invasive leading edge of keloids is higher than that in the surrounding skin: specifically, there is strong neovascularization and reddening at the edge that associates with the clinical symptoms of pain and pruritus. Moreover, these symptoms (and lesion growth in the case of small keloids) are improved by vasoconstrictive therapies.[1,2] By contrast, the center of keloids exhibits relatively few blood vessels and less reddening and fewer symptoms. In addition, histological studies suggest that the vascular lumens of the central keloid capillaries are flattened, and that this associates with an inadequate blood supply. As a result, Touchi et al suggested that the center of keloids is ischemic.[5] However, if that is the case, one would expect to see keloids develop into ischemic ulcers, which does not occur.

From the Department of Plastic, Reconstructive and Aesthetic Surgery, Nippon Medical School Hospital, Tokyo, Japan.

Received for publication August 23, 2021; accepted April 12, 2022.

DOI: 10.1097/GOX.0000000000004374

Disclosure: *The authors have no financial interest to declare in relation to the content of this article.*

To further improve our understanding of the role of blood vessels in keloids, we conducted the present study. First, we used near-infrared spectroscopy (NIRS) to examine the hemodynamics of keloids in situ; this device indicates the regional saturation of oxygen (rSO2) and the total hemoglobin index (T-HbI). Second, multidetector-low computed tomography (MDCT) was used to delineate the anatomy of the blood vessels around keloids. Third, excised keloid specimens were subjected to histology with optical, CD31 immunohistochemical, and electron microscopy.

Takeaways

Question: Our current understanding of keloid hemodynamics, the vessel anatomy around keloids, and the vascular architecture inside keloids remains very limited. It is unknown whether keloids are ischemic, congestion, or hyperemic.

Findings: Keloids may associate with congestion rather than ischemia.

Meaning: Methods that improve the blood circulation in keloids may be effective therapies.

PATIENTS AND METHODS

Ethics and Patient Recruitment

This experimental study included patients with keloids and healthy control subjects. The study was approved by the ethics committee of Nippon Medical School, Tokyo, Japan, and was conducted according to the Declaration of Helsinki. All subjects provided written informed consent to participate in the study.

Patients with anterior chest keloids and unscarred control subjects were recruited into the study in a convenience series. General inclusion criteria were Japanese ethnicity, age between 18 and 60 years, and lack of major diseases such as cancer or immunological disorders. Patients with anterior chest keloids were chosen to standardize the anatomical area that was being examined. The inclusion criterion for the NIRS and MDCT analyses on patients was a keloid that was 20 cm^2 or greater in size because pilot tests showed that these keloids had significantly different hemodynamics relative to the controls (data not shown). The inclusion criterion for the histological analyses on patients was a keloid that was 10 cm^2 or greater in size because it was more likely than smaller keloids to have a clearly demarcated leading edge and core.

Clinical Treatment of Keloids

All patients were treated according to our keloid treatment algorithm, the details of which were published recently.[2] The patients with 20 cm^2 or greater keloids were treated with total keloid extirpation, local flap surgery, and postoperative radiotherapy. The patients with smaller (10–19 cm^2) keloids were treated with total extirpation, Z-plasties, subcutaneous tension reduction suturing, and postoperative radiotherapy. Steroid plasters were applied if the slightest signs of recurrence were observed. None of the keloids recurred (follow-up duration >2 years). These treatments and their associated recurrence rates have been described extensively in our previous articles.[2,9,16–18]

Near-infrared Spectroscopy

NIRS was conducted on 20-cm^2 or greater anterior chest keloids by sequentially attaching the probe of a tissue oxygen saturation analyzer (Toccare, Astem Co, Ltd, Kanagawa, Japan) to 10–20 sites that were about 1–2 cm away from each other. The process was then repeated on the healthy skin around the keloid. An example of this process is shown in Figure 1. rSO2 and T-HbI were measured at each site three times, and the average value was calculated. rSO2 was expressed as % of maximal rSO2. T-HbI was expressed as the recorded value. In Figure 1, these values are indicated as %rSO2/T-HbI × 100; for example, 56/3 indicates 56% rSO2 and 0.03 T-HbI.

Multidetector-low Computed Tomography

Preoperative MDCT was conducted to detect perforators for skin flap surgery in patients with 20-cm^2 or greater anterior chest keloids. The Digital Imaging and Communications in Medicine (DICOM) viewer Osirix, ver 37 (Pixmeo, Bernex, Switzerland) was used to analyze the DICOM data taken by MDCT. Three analyses were conducted.

Histology

Patients with 10-cm^2 or greater anterior chest keloids underwent surgical resection. The margins and central areas of the excised keloids were fixed with 4% paraformaldehyde and 25% glutaraldehyde and stained with toluidine blue. Moreover, immunohistological staining of CD31 was performed by using a Vectastatin ABC kit and a 3,38-diaminobenzidine (DAB) kit (Vector Laboratory, Burlingame, Calif.). Healthy skin that was discarded from the same patients served as a control. The blood vessels in both tissues were then observed with histology with optical, CD31 immunohistochemical, and electron microscopy. Digital images of sequential fields in toluidine-stained normal skin and the leading edge and core of the keloids were obtained at 40× magnification. The blood vessels in five different fields in each slide were counted by two blinded observers and then averaged.

Statistics

Paired Student *t*-test was used to compare groups. Differences were considered significant when P values were less than 0.05. All statistical analyses were performed by using InStat, version 31 (GraphPad software, Inc, Calif.).

RESULTS

In total, 32 patients with keloids and three unscarred control volunteers were enrolled in this study. Their demographic and clinical details are shown in Table 1. Twenty patients had 20 cm^2 or greater anterior chest keloids. Of these, 10 underwent NIRS of their keloids and surrounding healthy skin for experimental purposes. The remaining 10

Fig. 1. NIRS-determined rSO2 and T-HbI values of keloids and their surrounding healthy skin NIRS were conducted at 1- to 2-cm intervals at 10–20 sites on both the keloid and the adjacent skin rSO2, and T-HbI were measured three times. The average values at each site were expressed as % maximal rSO2/T-HbI × 100. A representative example is shown.

patients underwent MDCT to find perforators for harvesting flaps. The three volunteers served as controls for the MDCT analyses. All underwent MDCT for experimental purposes. The remaining 12 keloid patients had 10- to 19-cm^2 keloids and underwent resection surgery, after which their excised keloids were subjected to histology. The healthy skin in dog ear that were resected after suturing served as the controls for these histopathology studies.

Table 1. Demographic and Clinical Characteristics of the Keloid Patients

Study	Age	Gender	Keloid Region	Cause	Size
NIRS	64	Masculine	Anterior chest	Cardiovascular surgery	≒80 cm^2
	25	Masculine	Anterior chest	Acne/folliculitis	≒30 cm^2
	75	Masculine	Anterior chest	Cardiovascular surgery	≒40 cm^2
	30	Feminine	Anterior chest	Acne/folliculitis	≒40 cm^2
	68	Masculine	Anterior chest	Cardiovascular surgery	≒50 cm^2
	36	Feminine	Anterior chest	Acne/folliculitis	≒70 cm^2
	58	Masculine	Anterior chest	Cardiovascular surgery	≒80 cm^2
	35	Masculine	Anterior chest	Acne/folliculitis	≒60 cm^2
	66	Masculine	Anterior chest	Cardiovascular surgery	≒40 cm^2
	73	Masculine	Anterior chest	Cardiovascular surgery	≒80 cm^2
MDCT	27	Feminine	Anterior chest	Acne/folliculitis	≒50 cm^2
	59	Masculine	Anterior chest	Acne/folliculitis	≒80 cm^2
	58	Masculine	Anterior chest	Acne/folliculitis	≒100 cm^2
	36	Feminine	Anterior chest	Acne/folliculitis	≒120 cm^2
	36	Masculine	Anterior chest	Acne/folliculitis	≒80 cm^2
	40	Masculine	Anterior chest	Acne/folliculitis	≒60 cm^2
	42	Masculine	Anterior chest	Acne/folliculitis	≒70 cm^2
	46	Masculine	Anterior chest	Acne/folliculitis	≒60 cm^2
	39	Masculine	Anterior chest	Acne/folliculitis	≒90 cm^2
	26	Feminine	Anterior chest	Acne/folliculitis	≒100 cm^2
Histology	26	Masculine	Scapular	Acne/folliculitis	≒20 cm^2
	68	Masculine	Anterior chest	Acne/folliculitis	≒20 cm^2
	58	Masculine	Anterior chest	Acne/folliculitis	≒15 cm^2
	36	Feminine	Abdomen	Abdominal surgery	≒20 cm^2
	73	Masculine	Anterior chest	Acne/folliculitis	≒20 cm^2
	50	Masculine	Anterior neck	Acne/folliculitis	≒15 cm^2
	49	Masculine	Anterior chest	Acne/folliculitis	≒20 cm^2
	36	Feminine	Scapular	Acne/folliculitis	≒15 cm^2
	45	Masculine	Scapular	Acne/folliculitis	≒15 cm^2
	42	Masculine	Anterior chest	Acne/folliculitis	≒20 cm^2
	38	Masculine	Anterior chest	Acne/folliculitis	≒15 cm^2
	28	Feminine	Anterior chest	Acne/folliculitis	≒20 cm^2

NIRS-determined rSO2 and T-HbI Values

Compared with the surrounding normal skin, the giant chest keloids in all 10 patients had significantly lower mean rSO2 (38.57% versus 61.08%, $P < 0.05$) and higher mean T-HbI values (0.059 versus 0.038, $P < 0.05$) (Fig. 2).

MDCT-determined Blood Vessel Anatomy in and around Keloids

The arteries within the giant chest keloids were all thin; thick arteries were seen only in the surrounding skin. Specifically, the keloids had on average 1.2 blood vessels with a lumen of 0.5 mm or greater compared with 6.3 in the skin surrounding the keloids.

All keloid patients also displayed alterations to the anatomy of the internal thoracic arteries and veins that respectively supply and drain the anterior chest skin. Thus, in all three healthy control subjects, the dominant perforator branches of the internal thoracic arteries and veins had an average diameter of 0.8 and 0.5 mm, respectively and all were located in the second intercostal space (ICS). By contrast, in the keloid patients, the dominant internal thoracic artery and vein perforators were all located in the first ICS and were much more dilated (average diameter:

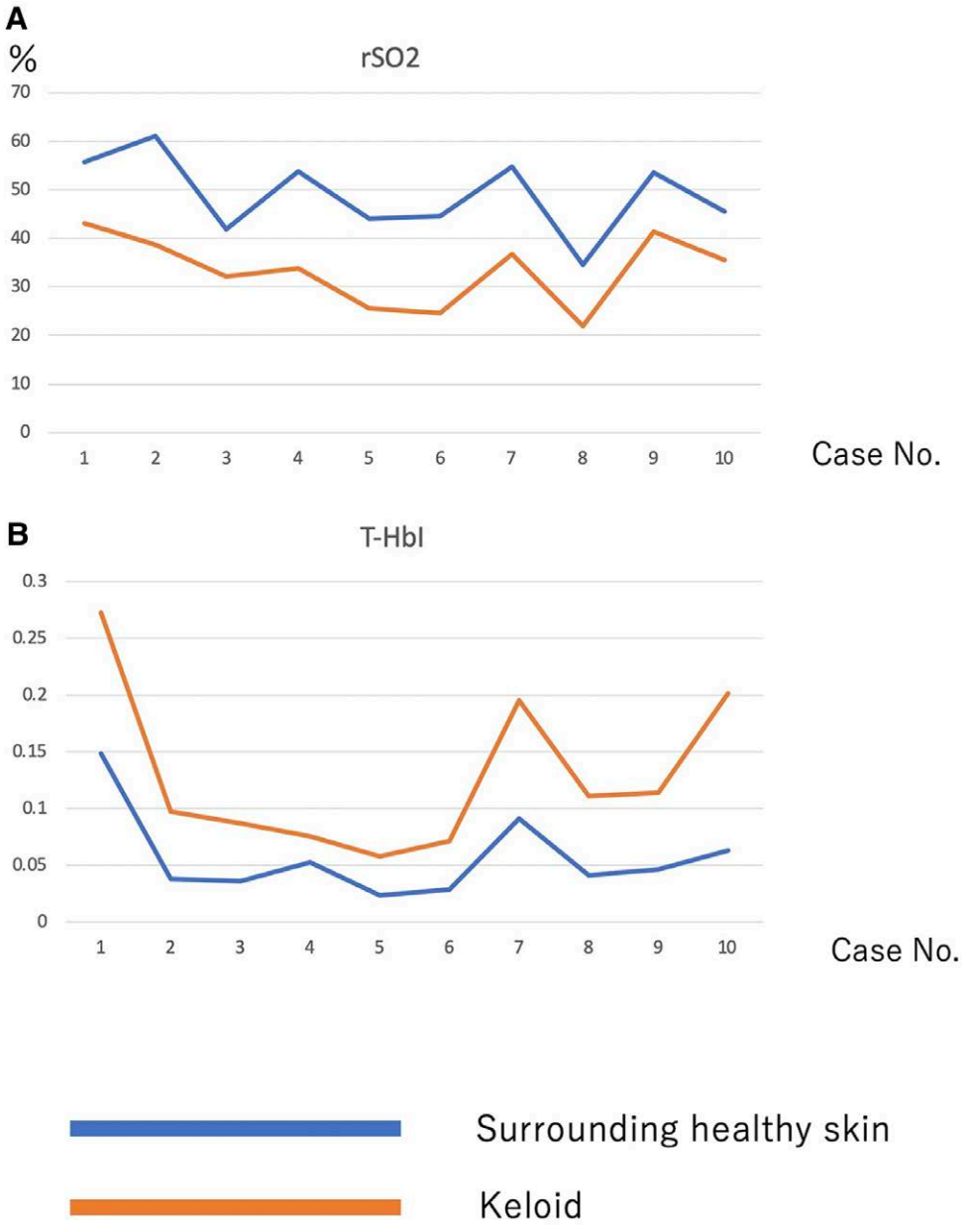

Fig. 2. NIRS-determined rSO2 and T-HbI values in 10 keloid cases. Compared with the healthy surrounding skin, the keloids had lower rSO2 (A) and higher T-HbI (B) values, which is suggestive of congestion in the keloids.

12 and 15 mm, respectively). In addition, the superficial vein that drains into the internal thoracic vein perforator in the first ICS was greatly expanded, and there was an arteriovenous shunt in the surface layer on both sides of the midline. Moreover, comparison of the surface and deep layers of the keloids indicated marked angiogenesis in the periphery and increased blood flow from the keloid center to the periphery.

A representative example of these findings is shown in Figure 3A. The anatomy of the patient's internal thoracic artery and vein perforators is depicted schematically in Figure 4. The MDCT images of this case are shown in Figure 3B, C: these images show the greatly dilated bilateral venous perforators in the first ICS at the periphery of the keloid and the thick surface vein running under the keloid. Figure 5 shows the MDCT details of the vasculature around and in the surface and deep layers of the keloid in the axial plane, including the dilated perforator vein (A in Fig. 5), the dilated subcutaneous vein running under the keloid (B), the blood vessels running into the keloid periphery (C), and the arteriovenous shunt at the periphery (D). Figure 6 schematically depicts Figure 5 and the normal vascular anatomy, and shows that the peripheral areas of the anterior chest keloid exhibit congestion that have led the superficial and especially perforator veins to dilate in an effort to improve the congestion.

Histopathological Analysis of the Vascular Structure in Extirpated Keloid Tissues

Microscopy after toluidine blue staining (Fig. 7) and CD31 immunostaining (Fig. 8) revealed significant neovascularization in the reddish leading edges of the keloids. There were significantly more blood vessels per high-power field (HPF) in the reddish leading edge of the keloid (mean, 13.9/HPF) than in the main body of the keloid (7.1/HPF, $P < 0.01$) or the normal skin in the dog ear (3.2/HPF, $P < 0.01$). The center of the keloid also tended to have more blood vessels than normal skin, although this did not achieve statistical significance ($P > 0.05$) (Fig. 7D).

Electron microscopy showed that while the reddish leading edges of the keloids had a large number of new blood vessels with 2–3 layers (data not shown), the lumens of many vessels inside the keloid centers appeared to be occluded or narrowed (Fig. 9). In some cases, the vascular structure was disrupted, and cellular components such as red blood cells and platelets appeared to be leaking into the vicinity. Notably, dense collagen fibers (keloidal collagen: KC) were inevitably found around the blood vessels (Fig. 9).

DISCUSSION

To increase our understanding of the role of blood vessels in keloid formation and progression, the present study examined the hemodynamics, surrounding vascular anatomy, and vascular histology of keloids. Our NIRS data suggested that keloids exhibit blood congestion, namely blood inflow is increasing and outflow is insufficient. This is because, as confirmed recently by multiple studies,[6–8] normal rSO2+high T-HbI, low rSO2+high T-HbI, and low rSO2+low T-HbI on NIRS respectively signify "initial congestion," "congestion," and "ischemia" states. Initial congestion is where blood inflow is increasing. In congestion, blood inflow is also increasing but outflow is insufficient. Ischemia is characterized by decreasing blood inflow with outflow also being small. Thus, our NIRS results suggest that keloids exhibit blood congestion. This notion was supported and expanded by our MDCT and histology data, as follows.

The High Blood Inflow in Keloids May Be Due to Both Vasodilation and Increased Angiogenesis at the Leading Edge

MDCT indicated that in keloid cases, the dominant perforators of the bilateral internal thoracic arteries were thicker than the dominant perforators in healthy subjects. They were also located at the leading edge of the keloids. Moreover, histology revealed considerable neovascularization in these edges but not the cores. The latter observation has been reported previously.[1,2] This suggested that there was great inflow of blood into the keloids.

These vascular patterns may reflect the potent and unrelenting inflammation in keloids, which concentrates in the leading edges as the lesion grows laterally. This inflammation is a key driver of keloid formation and progression. Although mild early inflammation is essential for normal wound healing, this stage is abnormally strong in keloid cases and does not subside. This may reflect, at least in part, local tension on the wound edges: keloids predominate on high-tension body sites and tend to grow in the direction of the prevailing stress forces.[9–12] It is thought that this local tension promotes vascular hyperpermeability and the resulting powerful influx of inflammatory cells; the inflamed nature of the tissue plus the ongoing skin tension then pathologically activate fibroblasts, which lay down excessive collagen, thereby causing scar thickening and stiffening.[9–12] The stiffening in turn makes the endothelial and inflammatory cells and fibroblasts in the scar more susceptible to the tension at the scar edges; this results in increased angiogenesis and inflammation at the scar margins, stimulation of the fibroblasts in these regions, and ultimately, invasive growth of the scar into the adjacent healthy skin.[10]

The Blood Outflow in Keloids May Be Insufficient because of Vascular Degeneration in the Keloid Center

MDCT and histology showed that there were few blood vessels in the keloid center compared with the margins and that the vessels that were present were narrowed, occluded, and even disrupted. These observations suggest that the blood vessel architecture in the keloid center has broken down. This means that in the keloid center, blood flowing from the surface of the keloid skin cannot be removed and instead stagnates. This is further supported by the MDCT findings, which showed strong dilation of the venous perforators at the keloid margin and the superficial vein running under the scar: these features suggest the tissue is trying hard to drain the blood from the destroyed keloid center.

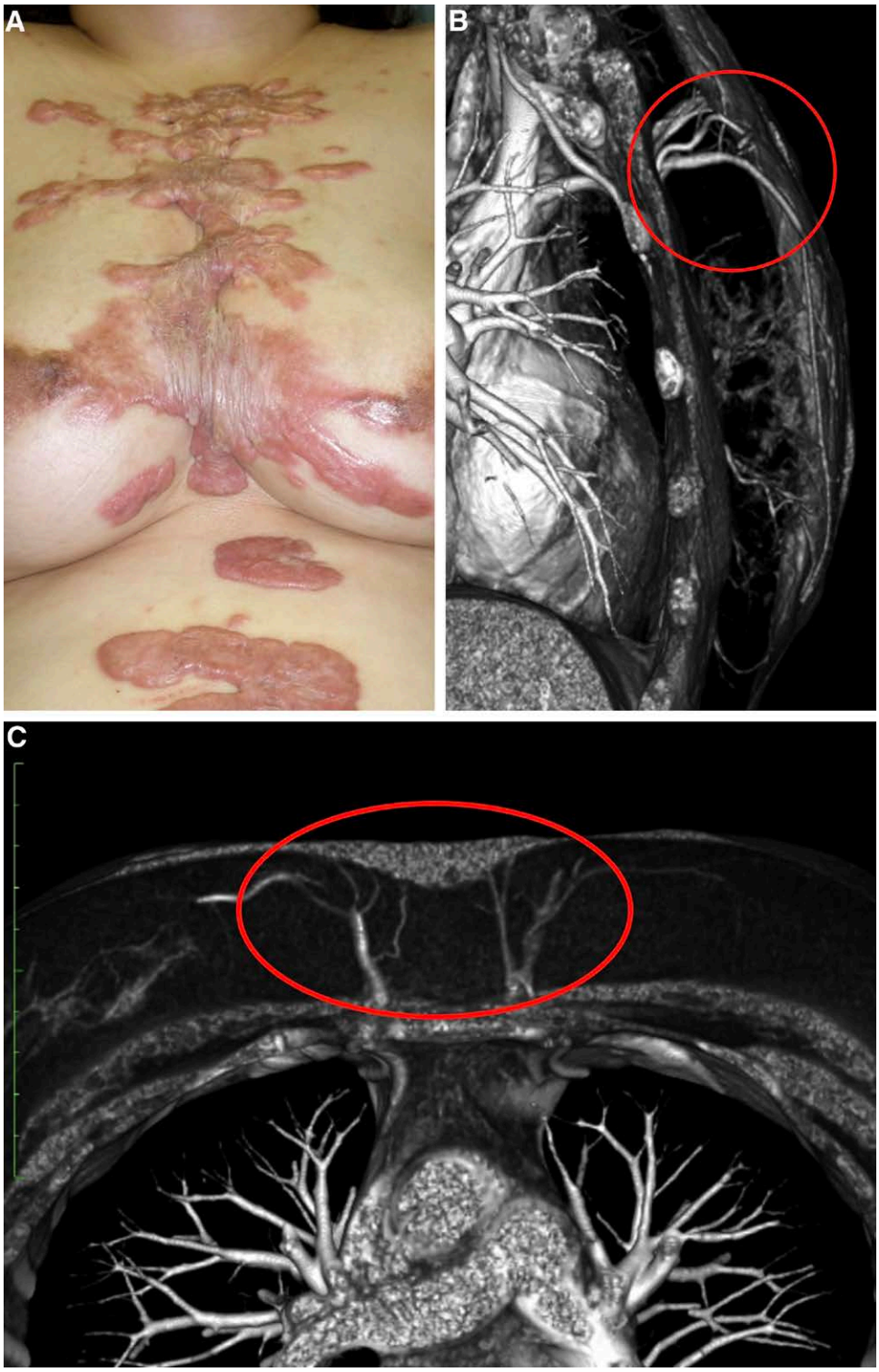

Fig. 3. A representative keloid case that underwent MDCT analysis. A, The clinical appearance of the keloid. MDCT views in the axial (B) and horizontal (C) planes indicate the internal thoracic perforating artery and vein in the first intercostal space and the superficial vein under the keloid. The veins exhibit strong dilation.

This is also supported by the fact that keloids associated with anatomical alterations in their surrounding vasculature[13,14]: the dominant perforators of the internal thoracic arteries were all located in the first ICS, whereas they were located in the second ICS in healthy subjects. This may reflect the strong metabolic demands of the keloid and its location.

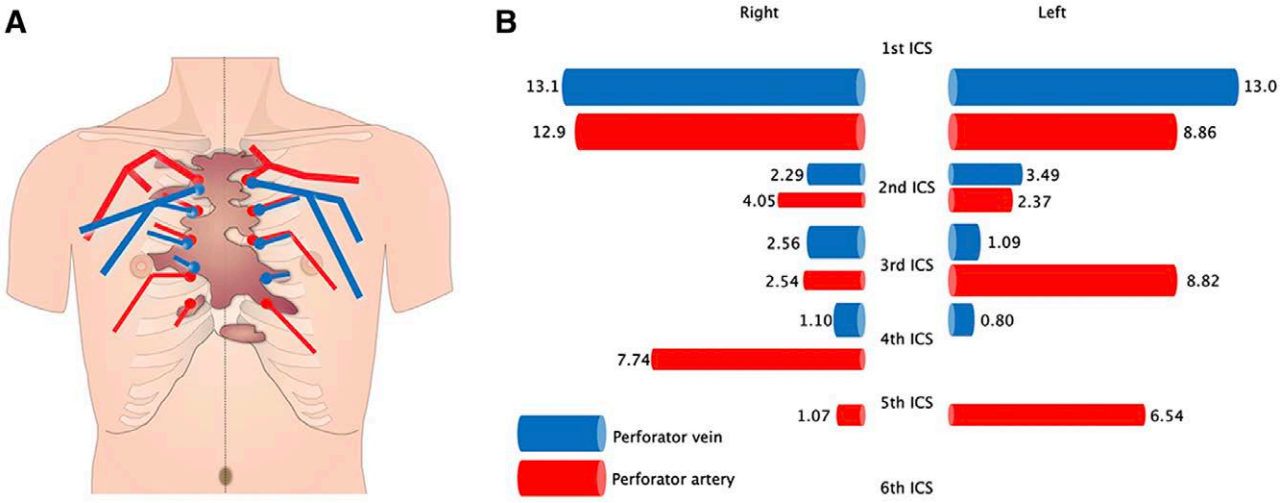

Fig. 4. Schematic depiction of the MDCT-determined anatomy of the bilateral internal thoracic artery and vein perforators in the representative keloid case shown in Figure 3. The course and thickness of the perforators are shown in A. The keloid is depicted in brown. The length (in cm) of the perforators in the first to sixth ICS is shown in B. The relative thickness of these vessels is indicated schematically.

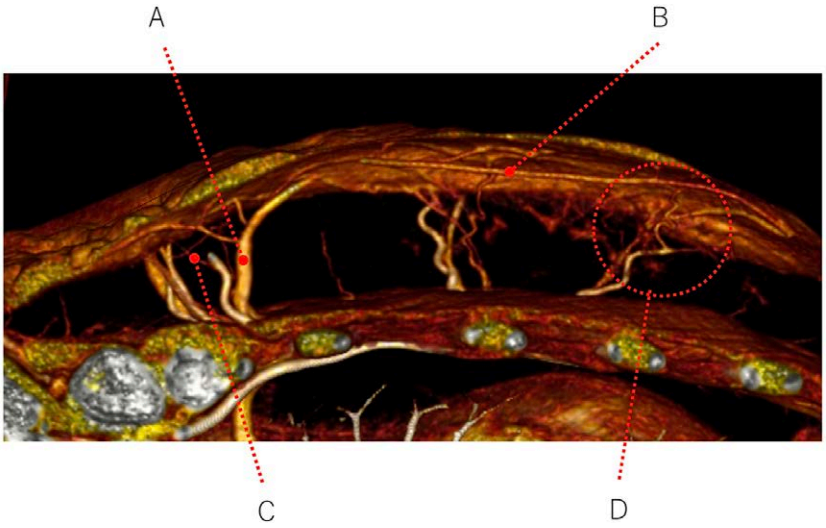

Fig. 5. A closer view of the MDCT image obtained in the axial plane from the representative keloid case shown in Figure 3. The blood vessels feeding and draining the keloid can be seen. They include the dilated perforator vein (A), the dilated subcutaneous vein running directly under the keloid (B), the blood vessels in the surrounding normal skin that are entering and leaving the keloid (C), and the arteriovenous shunt (D).

It was notable that the vascular injuries in the keloid center associated with strong collagen fiber accumulation. It is possible that the vascular degeneration prevents sufficient oxygen from reaching the tissue and that the resulting hypoxia promotes collagen production and makes it difficult to break the existing collagen down.[15,16] The notion that keloids exhibit hypoxia is supported by a study by Ueda et al, which showed that keloids produce ATP via anaerobic metabolism.[4] The collagen accumulations could potentially also have a converse effect, namely they disrupt the existing blood vessels. Both mechanisms could operate together, creating a vicious circle that devastates the vascular architecture in the keloid center and blocks blood outflow.

Keloids Exhibit Congestion rather than Ischemia

Touchi et al suggested that because the center of keloids have lower vascular density than the margins, this part of the scar is ischemic[5] (ie, blood inflow is decreasing and outflow is also small). We propose that the term "congestion" may be more reflective of the overall physiological condition of keloids. To illustrate our point, we show a chest keloid in Figure 10. This keloid runs along the horizontal axis of the chest and bears a strongly reddened scar leading edge (Fig. 10A), a more mildly inflamed scar leading edge at the other end, less red central parts (Fig. 10B), a maturing scar in the center (Fig. 10C), and normal skin around the whole lesion (Fig. 10D). As indicated by its rising number of blood vessels, rising hemoglobin, and

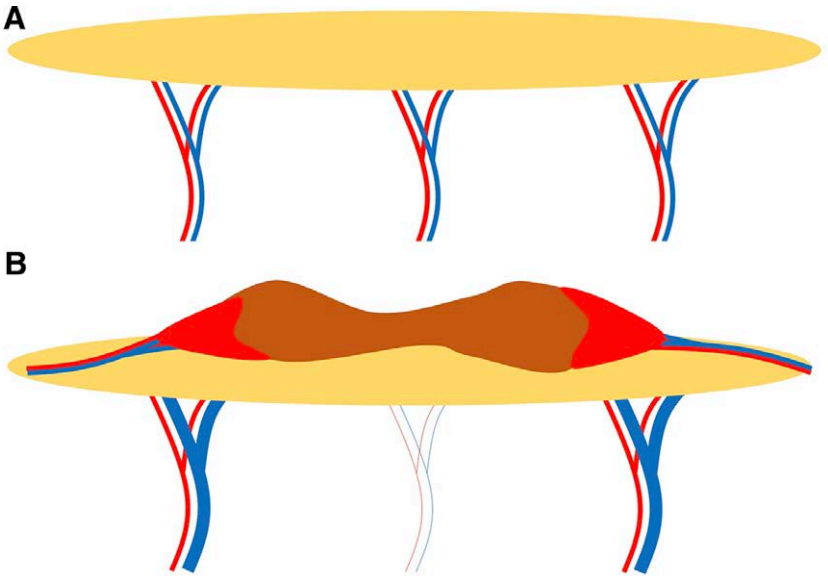

Fig. 6. Schematic depiction of the blood vessels around and below the healthy skin (A) and the keloid (B) in the representative case shown in Figure 3. The red areas at the margin of the keloid indicate congestion.

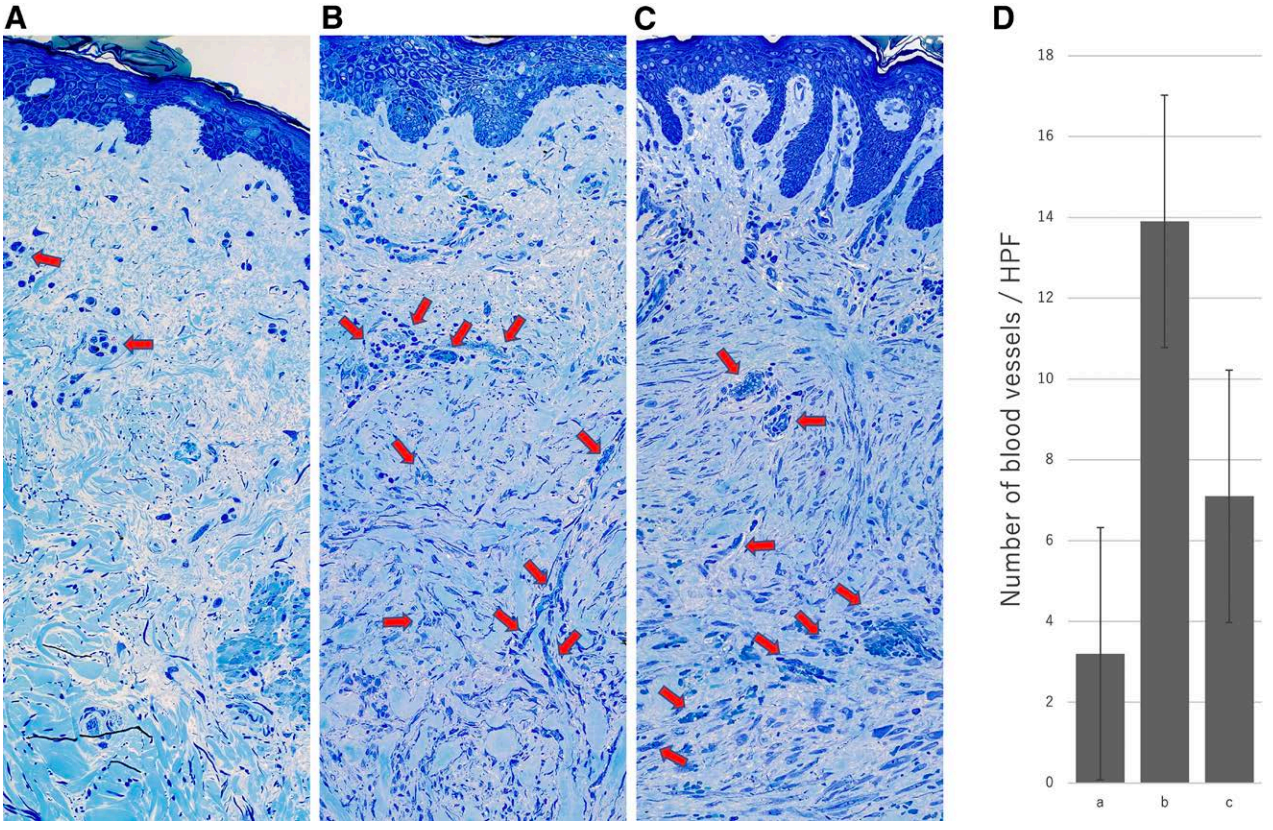

Fig. 7. Optical microscopic view of normal skin (A) and the reddish leading edge (B) and main body (C) of an extirpated toluidine-blue-stained keloid. A representative sample is shown. The arrows show the blood vessels. The number of blood vessels per high-power field (HPF) is shown on the graph (D).

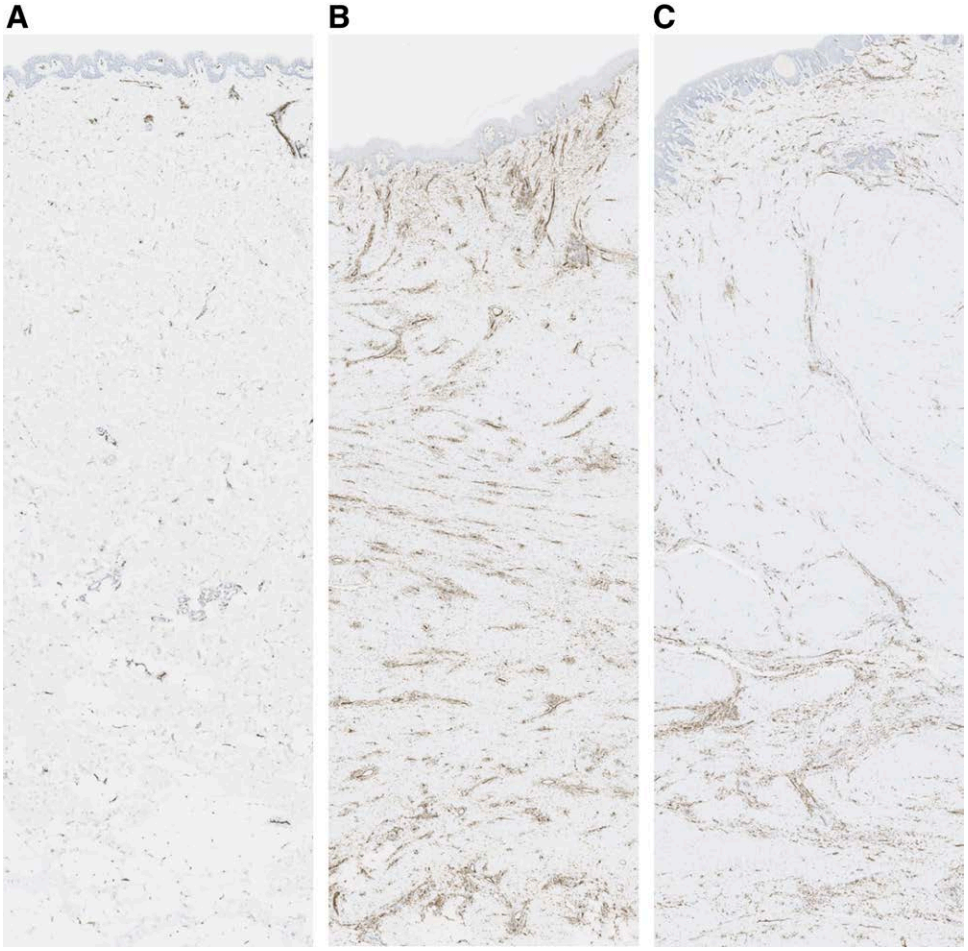

Fig. 8. CD31-stained endothelial cells in normal skin (A) and the reddish leading edge (B) and main body (C) of an extirpated keloid. A representative sample is shown.

decreasing oxygen, congestion is highest at the keloid leading edge. The congestion then gradually decreases toward the center of the scar, as shown by the unchanging number of blood vessels, a smaller rise in hemoglobin, and an unchanged decrease in oxygen. Congestion is absent in the maturing scar, which exhibits decreasing numbers of blood vessels and a normal balance of hemoglobin and oxygen. Thus, the term ischemia is not accurate in any situation here, including in the mature scar: although the blood flow in the mature scar seems to be reduced compared with surrounding healthy skin, this is "relative ischemia" rather than "absolute ischemia."

The possibility that keloids are in a congested state rather than in an ischemic state is supported by the fact that keloids do not develop into ischemic ulcers (although hair follicles occluded by the keloid do sometimes develop into infected ulcers). It should be noted here that the normal wound healing process also involves neovascularization and tissue remodeling that associates with some congestion. However, this congestive state will subside quickly as long as the inflammation resolves. By contrast, in keloids, the inflammation continues and escalates, resulting in a long-term congestive state.

Study Limitations

This experimental study employed 10 keloid patients each for the NIRS and MDCT analyses, respectively. These relatively small patient numbers reflect the rarity of patients with large keloids, which were selected because such extremely large keloids would best demonstrate hemodynamic differences relative to the controls. In addition, our MDCT study included only three healthy control subjects. This reflects the fact that MDCT is not without risk. Nonetheless, our results should be confirmed with a much larger case series.

CONCLUSIONS

Our NIRS, MDCT, and histology studies suggest that the vascular architecture breaks down in the keloid center, leading to central blood stagnation. This may be partnered by massive inflow of blood into the keloid via increased angiogenesis at the leading edges and thickening of the arterial perforators. In an attempt to rectify this congested state, the surrounding veins may dilate. Thus, keloids may associate with congestion rather than with ischemia. These findings suggest that improving the congestion in keloids could be a viable therapeutic strategy for these lesions. This may be a significant finding

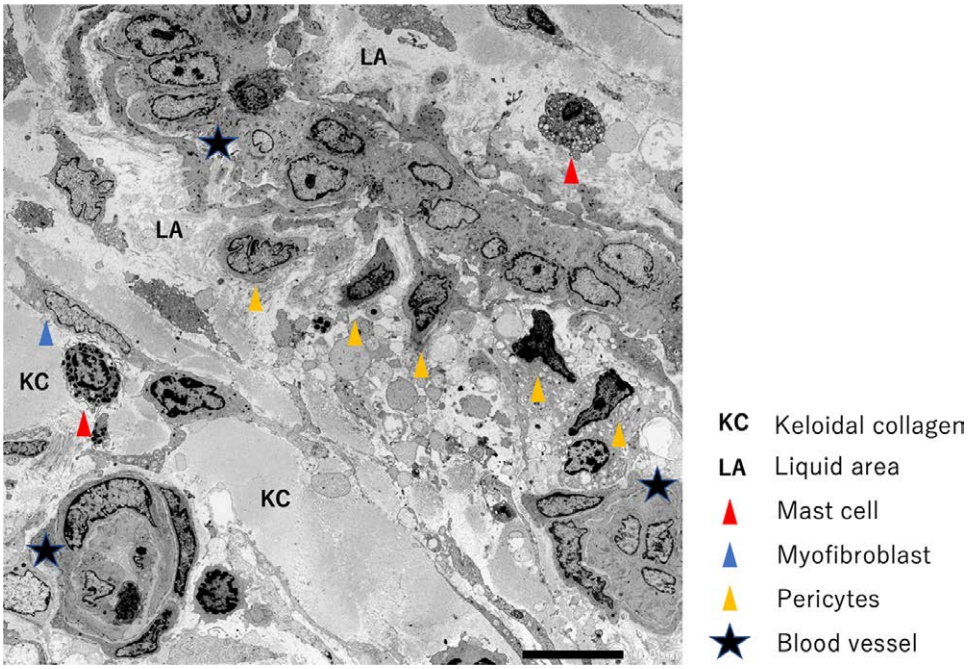

Fig. 9. Electron microscopic view of the tissue within a representative keloid. The lumens of many of the vessels inside the main body of the keloid appear to be occluded or narrowed (star). Although each blood vessel was covered with a basement membrane, it had high vascular permeability and a liquid area containing blood components and fibrin could be detected. There was KC in the vicinity.

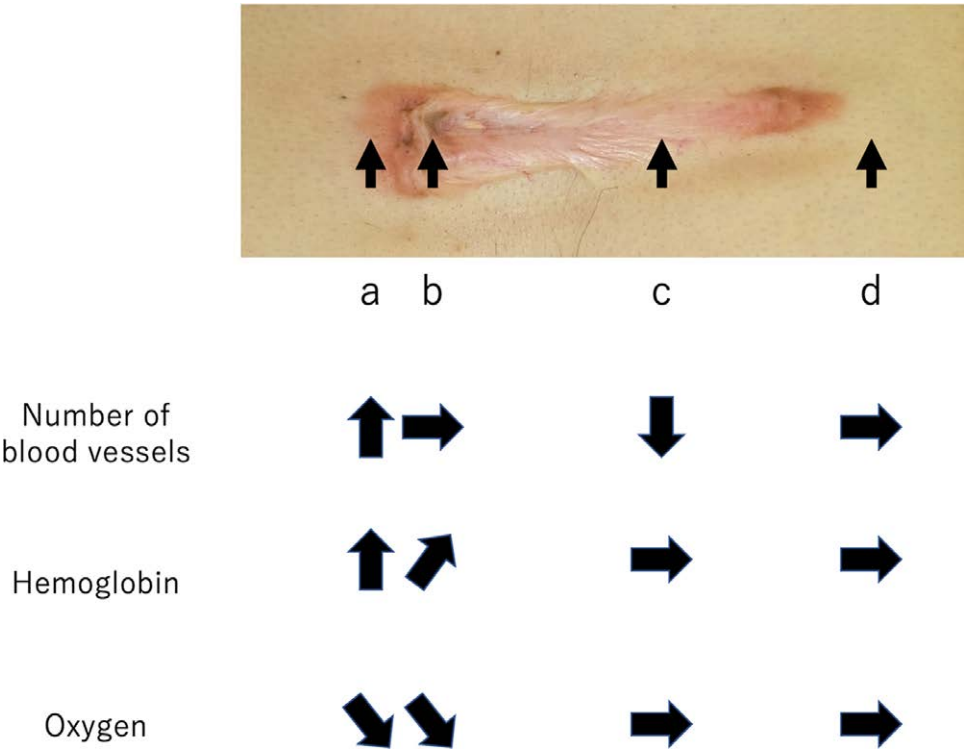

Fig. 10. Schematic depiction illustrating the relative number of blood vessels and hemoglobin and oxygen levels in the keloid leading edge (a), the keloid center (b), the mature scar (c), and the normal surrounding skin (d) of a patient with a chest wall keloid These values indicate high congestion in the leading edge, lower congestion in the center, and relative (but not absolute) ischemia in the mature scar compared with the surrounding skin.

because although recent studies have greatly improved our understanding of keloidogenesis,[17–20] the mechanisms that underlie keloid progression and could be targeted therapeutically remain to be elucidated.

Rei Ogawa, MD, PhD, FACS
Department of Plastic, Reconstructive and Aesthetic Surgery
Nippon Medical School
1-1-5 Sendagi Bunkyo-ku
Tokyo 113-8603, Japan
E-mail: r.ogawa@nms.ac.jp

REFERENCES

1. Ogawa R. Keloid and hypertrophic scars are the result of chronic inflammation in the reticular dermis. *Int J Mol Sci.* 2017;18:E606.
2. Ogawa R, Dohi T, Tosa M, et al. The latest strategy for keloid and hypertrophic scar prevention and treatment: the Nippon Medical School (NMS) protocol. *J Nippon Med Sch.* 2021;88:2–9.
3. Kurokawa N, Ueda K, Tsuji M. Study of microvascular structure in keloid and hypertrophic scars: density of microvessels and the efficacy of three-dimensional vascular imaging. *J Plast Surg Hand Surg.* 2010;44:272–277.
4. Ueda K, Yasuda Y, Furuya E, et al. Inadequate blood supply persists in keloids. *Scand J Plast Reconstr Surg Hand Surg.* 2004;38:267–271.
5. Touchi R, Ueda K, Kurokawa N, et al. Central regions of keloids are severely ischaemic. *J Plast Reconstr Aesthet Surg.* 2016;69:e35–e41.
6. Astem. User's manual of the oximetry with sensor attached to examiner's finger: Toccare. Available at https://astem-jp.com/wp-content/uploads/2021/10/toccare_en.pdf. Accessed May 22, 2022.
7. Ozawa J, Watanabe T, Ito M, et al. Defining the reference range of regional cerebral tissue oxygen saturation using a new portable near-infrared spectroscopy device for term infants. *Early Hum Dev.* 2020;141:104941.
8. Tovedal T, Jonsson O, Zemgulis V, et al. Venous obstruction and cerebral perfusion during experimental cardiopulmonary bypass. *Interact Cardiovasc Thorac Surg.* 2010;11:561–566.
9. Ogawa R. Mechanobiology of scarring. *Wound Repair Regen.* 2011;19(Suppl 1):s2–s9.
10. Ogawa R, Akaishi S, Kuribayashi S, et al. Keloids and hypertrophic scars can now be cured completely: recent progress in our understanding of the pathogenesis of keloids and hypertrophic scars and the most promising current therapeutic strategy. *J Nippon Med Sch.* 2016;83:46–53.
11. Harn HI, Ogawa R, Hsu CK, et al. The tension biology of wound healing. *Exp Dermatol.* 2019;28:464–471.
12. Dohi T, Padmanabhan J, Akaishi S, et al. The interplay of mechanical stress, strain, and stiffness at the keloid periphery correlates with increased Caveolin-1/ROCK signaling and scar progression. *Plast Reconstr Surg.* 2019;144:58e–67e.
13. Matsumoto NM, Peng WX, Aoki M, et al. Histological analysis of hyalinised keloidal collagen formation in earlobe keloids over time: collagen hyalinisation starts in the perivascular area. *Int Wound J.* 2017;14:1088–1093.
14. Ogawa R, Akaishi S, Izumi M. Histologic analysis of keloids and hypertrophic scars. *Ann Plast Surg.* 2009;62:104–105.
15. Lei R, Li J, Liu F, et al. HIF-1α promotes the keloid development through the activation of TGF-β/Smad and TLR4/MyD88/NF-κB pathways. *Cell Cycle.* 2019;18:3239–3250.
16. Kang Y, Roh MR, Rajadurai S, et al. Hypoxia and HIF-1α regulate collagen production in keloids. *J Invest Dermatol.* 2020;140:2157–2165.
17. Betarbet U, Blalock TW. Keloids: a review of etiology, prevention, and treatment. *J Clin Aesthet Dermatol.* 2020;13:33–43.
18. Huang C, Ogawa R. Keloidal pathophysiology: current notions. *Scars Burn Heal.* 2021;7:2059513120980320.
19. Ogawa R, Akita S, Akaishi S, et al. Diagnosis and treatment of keloids and hypertrophic scars—Japan scar workshop consensus document 2018. *Burns Trauma.* 2019;7:39.
20. Ogawa R. The most current algorithms for the treatment and prevention of hypertrophic scars and keloids: a 2020 update of the algorithms published 10 years ago. *Plast Reconstr Surg.* 2022;149:79e–94e.